The P940 Upstream Magnetic Spectrometer

Hogan Nguyen

March 22, 2005

Abstract

This document presents the proposed layout of the P940 Upstream Magnetic Spectrometer, the required performance, and simulation results. The simulation includes important effects such as multiple scattering, chamber response, and effects related to multiple tracks in a 230 MHz secondary beam.

1 Introduction and Requirements

The Upstream Magnetic Spectrometer (UMS) is designed to measure the momentum and trajectory of the K^+ as it enters the decay volume. The UMS is used together with the K^+ velocity measurement from the Kaon Rich (Krich), the measurement of the π^+ trajectory and momentum from the Downstream Magnetic Spectrometer (DMS) and Pion Rich (Prich), to achieve the best possible recoil (missing) mass measurement. The expression for the mass recoiling against the π^+ in the K^+ CM frame is:

$$M^2_{miss} = M_K^2(1 - \frac{p_\pi}{p_K}) + M_\pi^2(1 - \frac{p_K}{p_\pi}) - p_K p_\pi \theta^2 \tag{1}$$

where θ is the angle between the K^+ and π^+ vectors in the lab frame. The missing mass reconstruction is used to reject (kinematically) the dominant 2-body decay backgrounds: $K\pi2$ and $K\mu2$.

Of these two, the $K\pi2$ background is more troublesome. This is because the M_{miss}^2 of the $K\pi2$ background overlaps substantially with M_{miss}^2 of the $\pi^+\nu\bar{\nu}$ signal.[1] On the other hand, the photon veto system is expected to reject the π^0 in $K\pi2$ decays at the 10^{-7} level. The relative branching ratio between the signal and $K\pi2$ background is expected to be $3.3 \cdot 10^{-10}$.

We can now estimate the kinematic rejection of the $K\pi2$ background needed for a S/N=10 in 'Region-I'. The detector geometrical acceptance to the π^+ is similar for $K\pi2$ and $\pi^+\nu\bar{\nu}$ decays. On the other hand, the kinematical acceptance of $\pi^+\nu\bar{\nu}$ is about 16% in Region-I. Therefore, to achieve a S/N $= 10$, the kinematical acceptance to $K\pi2$ needs to be less than $5.28 \cdot 10^{-5}$. As we will see later in this document, the simulation shows that the UMS design meets this requirement. For the simulation of the π^+ response, only gaussian detector responses were simulated (i.e. no multiple scattering in DMS or Prich). This is because we wish to study the imperfections of the UMS in isolation.

2 Detector Technology

A challenge for the UMS is to track 10 MHz of kaons in an environment of 220 MHz of other charged particles. The tracking chambers must be sufficiently thin to minimize multiple scattering and interactions. The detector must be efficient to tracks in this high-rate environment, and the response must be sufficiently fast. We plan to use technology similar to the Kabes[1] system developed by the Saclay group for NA48/2. These are gas-based TPC's where the gain stage is performed by a single micromegas mesh[2].

Figure 1 shows the principle of operation. A single UMS chamber consists of a 10 cm

---

[1] The M_{miss}^2 of $K\mu2$ events, using the hypothesis that the μ^+ charged daughter is a π^+, is substantially far away from the M_{miss}^2 signal. In addition, the μ^+ is identified by the Prich and DMS combination, and independently by the Muon Veto System (MVS)

x 10 cm x10 cm volume of gas such as CF_4-ethane. Since the P940 beam consists of nearly parallel tracks, we arrange the beam to enter through the center of this cube and parallel to the z-axis. The ionized electrons are drifted by a uniform E-field (parallel to the x-axis) towards a micromegas mesh and an anode strip plane. The anode strip pitch is 800 μm. The gap between the mesh and anode strip is 25 μm.
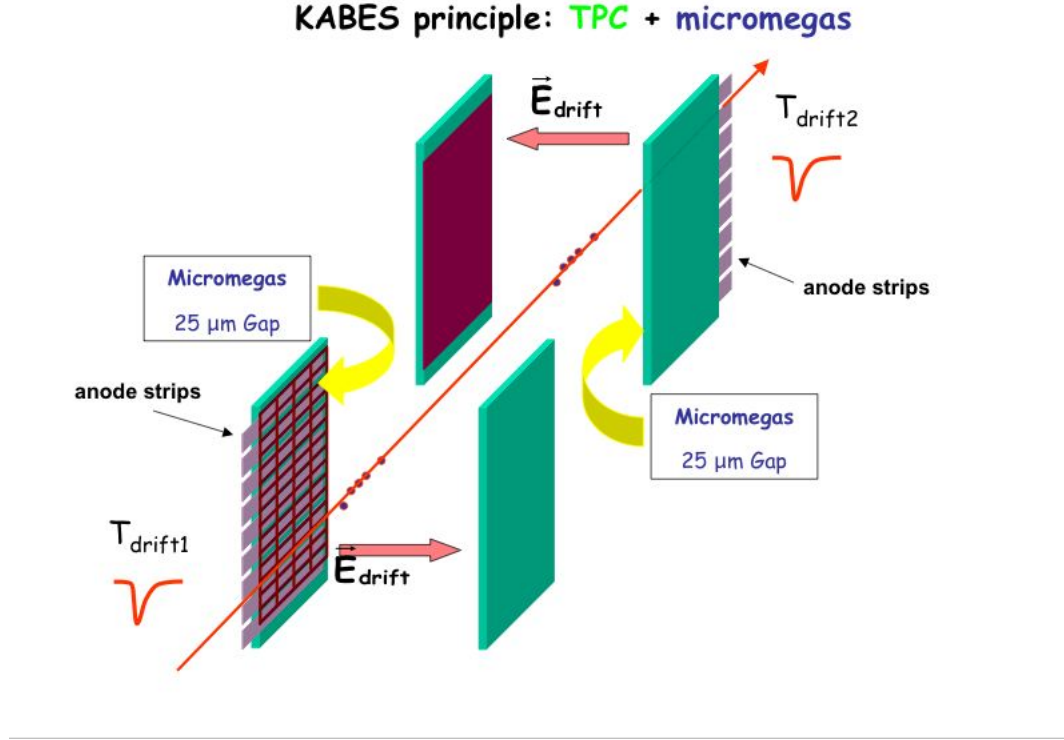

Fig. 1. The operating principle of the NA48/2 Kabes device.

This design has several significant advantages, as is summarized in the following few paragraphs. The TPC concept allows for a 1-d space and time measurement derived from a single hit, allowing for a relatively compact electronics readout system. The chambers are relatively thin, as the tracks traverse two 1-mil kapton windows and 10 cm of CF4-ethane.

Because we arrange the beam to be parallel to the anode strip direction, the ionization

electrons of a given track will drift into the mesh almost *simultaneously*, modulo gas diffusion. This is very different than the situation in conventional wire chambers in which ionization clusters drift times are vastly different. Therefore, a track traversing 10 cm of CF_4-ethane will deposit about 500 electrons that drift coherently onto the micromegas mesh.

The gas amplification occurs in the 25 μm gap between the micromegas mesh and the anode strip plane. This process produces intrinsically short pulses. The anode strip current consists of a fast electron current, and a slower ion-return current. However, in the micromegas amplification process, ions travel about 25 μm. Therefore, unlike wire drift chambers, where the ions typically travel a distance of order millimeters to centimeters, ions are swept out of the gain region rather quickly. Figure 2 shows a pulse shape from the NA48/2 Kabes.
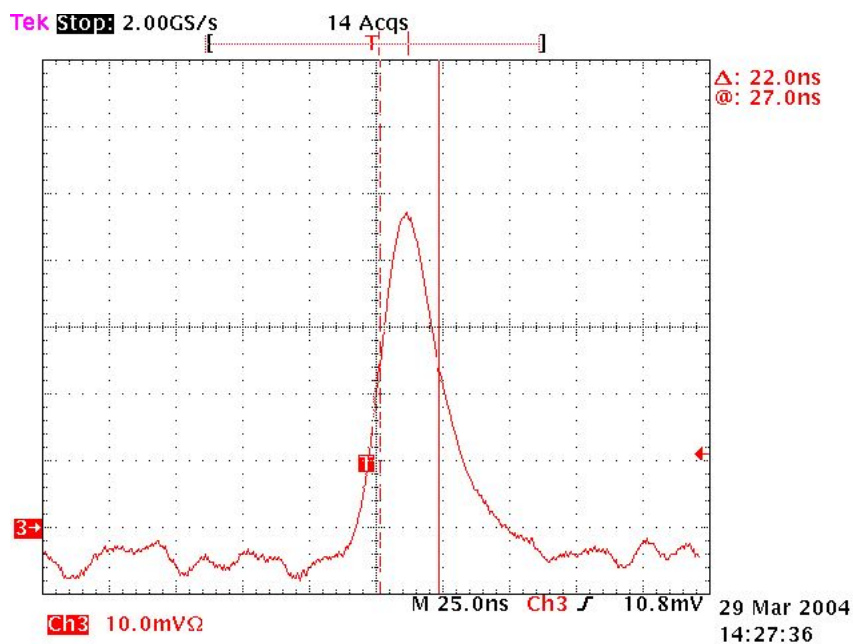

Fig. 2. Pulse shape response of a 25 μm gap micromegas mesh to an an Fe^{55} source[3].

4

3 Detector Layout

The UMS consists of 10 chambers (figure 3): 6 and 4 chambers on either side of a dipole analysis magnet. The analysis magnet is part of an achromat, where the bendviews are in the vertical direction. The chambers are oriented such at the ionization electrons drift in the horizontal view. The odd-numbered chambers drift electrons in the +x direction, the even-numbered chambers drift in the -x direction. The time when a chamber hit is observed depends on the event time (i.e. track arrival time at the chamber), and on the drift time of the ionization electrons (i.e. the x-coordinate). In a single chamber, it is not possible to resolve this ambiguity. However, in an arrangement of chambers with alternating drift directions, this ambiguity can be resolved. A fit can be made to hits for the follow 6 parameters: 5 track spatial parameters consisting of x_0, θ_x, y_0, θ_y, p, and the event time t_0.

The beam and achromat are important for the UMS performance and reconstruction. To first order approximation, the beam enters the achromat with a momentum bite of 37-53 GeV and has zero divergence. The pencil beam is dispersed by the achromat as it goes through the UMS chambers, and then is recombined back into a pencil beam by the achromat before it enters the Krich. This reduces the single rate on the UMS anode strips. Since the beam has almost zero divergence, there is a strong correlation between the track momentum and the strips that are hit. As will be shown later, this is useful in the pattern recognition.

It is important to minimize the material upstream of the vacuum decay volume. Each pair of UMS chambers consists of 5 1-mil kapton windows and 20 cm of CF_4-ethane. Each helium bag and the Krich have 2 1-mil kapton windows. The vacuum decay volume has a 23-mil kevlar window. The material content from the first UMS chamber to the vacuum decay volume is $16.5 \cdot 10^{-3}$ X_0 and $11.6 \cdot 10^{-3}$ λ_0. Figure 4 shows the relative material contributions.
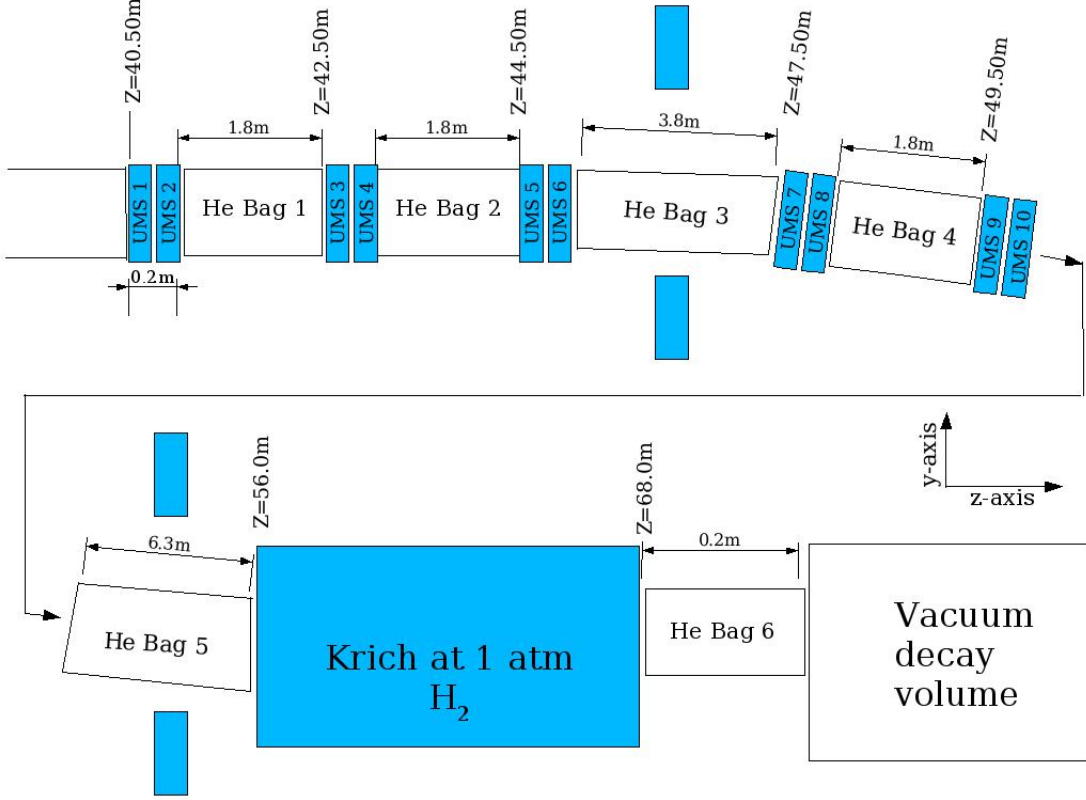
Fig. 3. Layout of the detectors upstream of the vacuum decay volume. The dipole magnets shown are the last two magnets of an achromat. The figure is not drawn to scale.

4 Simulations and Results

We use two simulation packages, described in the following two sections, to predict the performance of the UMS. In particular, we check the response of the UMS to $K\pi2$ events and see how the detector imperfections contribute to $K\pi2$ background. In these packages, the other tracking detectors (Krich, DMS, Prich) are simulated as having gaussian resolution functions. And multiple scattering was not simulated for the daughter π^+. This is done in order to study the UMS in isolation.
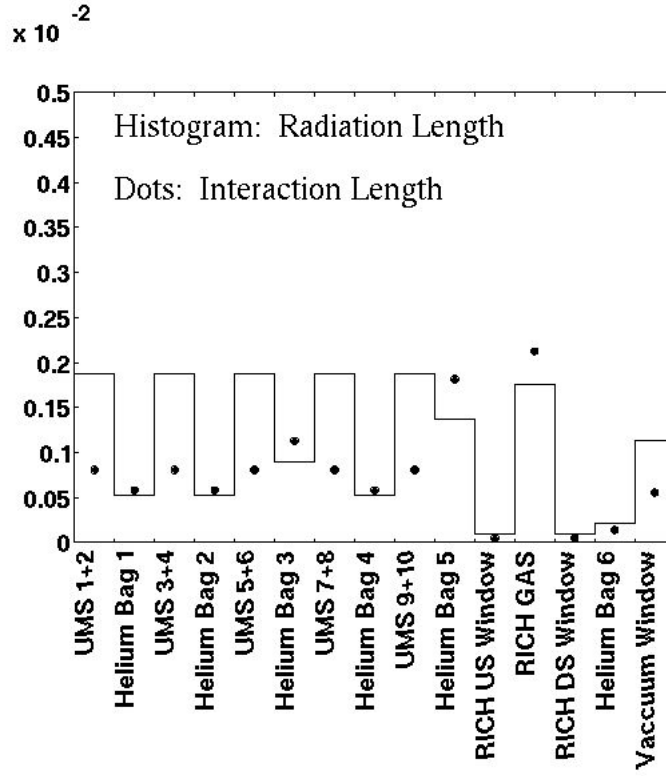
Fig. 4. The contribution of material in the detectors upstream of the vacuum decay volume. The histogram (dots) indicate the amount of radiation (interaction) length. The total radiation and interaction length is $16.5 \cdot 10^{-3} \; X_0$ and $11.6 \cdot 10^{-3} \; \lambda_0$ respectively.

4.1 Multiple Scattering in the Upstream Detectors

A simulation package, based on GEANT-3 and FLUKA, is used to predict multiple scattering of the K^+ tracks in the material from UMS-1 to the window (made of kevlar) upstream of the vacuum decay volume. The K^+ decay to $\pi^+\pi^0$ is subsequently generated in the vacuum decay volume. The scattering includes both multiple coulomb and hadronic scattering, and the production of secondaries. In the case where secondaries have been generated, the secondaries are traced through the detector without any energy deposits. This is conservative, as we expect to have some sensitivity to vetoing the secondaries.

7

The amount of material simulated is shown in figure 4. Single K^+ tracks are traced through this material. There is no attempt to simulate the UMS time response and pattern recognition. The response of the UMS detectors (i.e. the UMS hits) are simply the actual x and y positions of the tracks smeared in a gaussian fashion by 140 μm in y (bendview), and 100 μm in x (non-bendview). The UMS track hits are processed by a 5 parameter fit to extract x_0, y_0, θ_x, θ_y, P_K, and a fit χ^2.

Figure 5 shows the K^+ angular and momentum resolutions, which are nearly constant over the range of 37-53 GeV/c. The tracks were selected to have a reduced $\chi^2 < 4$. The figure also shows the simulation without scattering. As we will see later, events in the non-gaussian tail are due mainly to scattering in the material contained in UMS-9 to the vacuum window. The scatters that occur in the region between UMS-1 to UMS-8 are rejected by the requirement on track reduced χ^2. The events that remain are scatters that cannot be discriminated by this χ^2 requirement.

On the other hand, scatters occurring in the region from UMS-9 to the vacuum window can be suppressed by requiring that the K^+ and π^+ tracks form a good decay vertex. The good-vertex variable is the distance-of-closest-approach (DOCA) between the reconstructed K^+ and π^+ tracks. For scatters, DOCA can be inconsistent with that of a good vertex since the K^+ track direction was misreconstructed. If the decay plane, defined as the plane that contains both K^+ and π^+ tracks, coincides with the scattering plane, then DOCA cannot be used to reject these scatters. Figure 6 shows the DOCA resolution, with and without scattering simulation. This mechanism was studied and documented in the CKM proposal.

Regarding the upstream detectors, it is important to identify the main differences between P940 and CKM. Each P940 UMS chamber is about 1/2 the material of a CKM UMS chamber. However, there is no plan currently to have a Kaon Entrance Angle Tracker (KEAT), which would have been installed immediately upstream of the vacuum window.
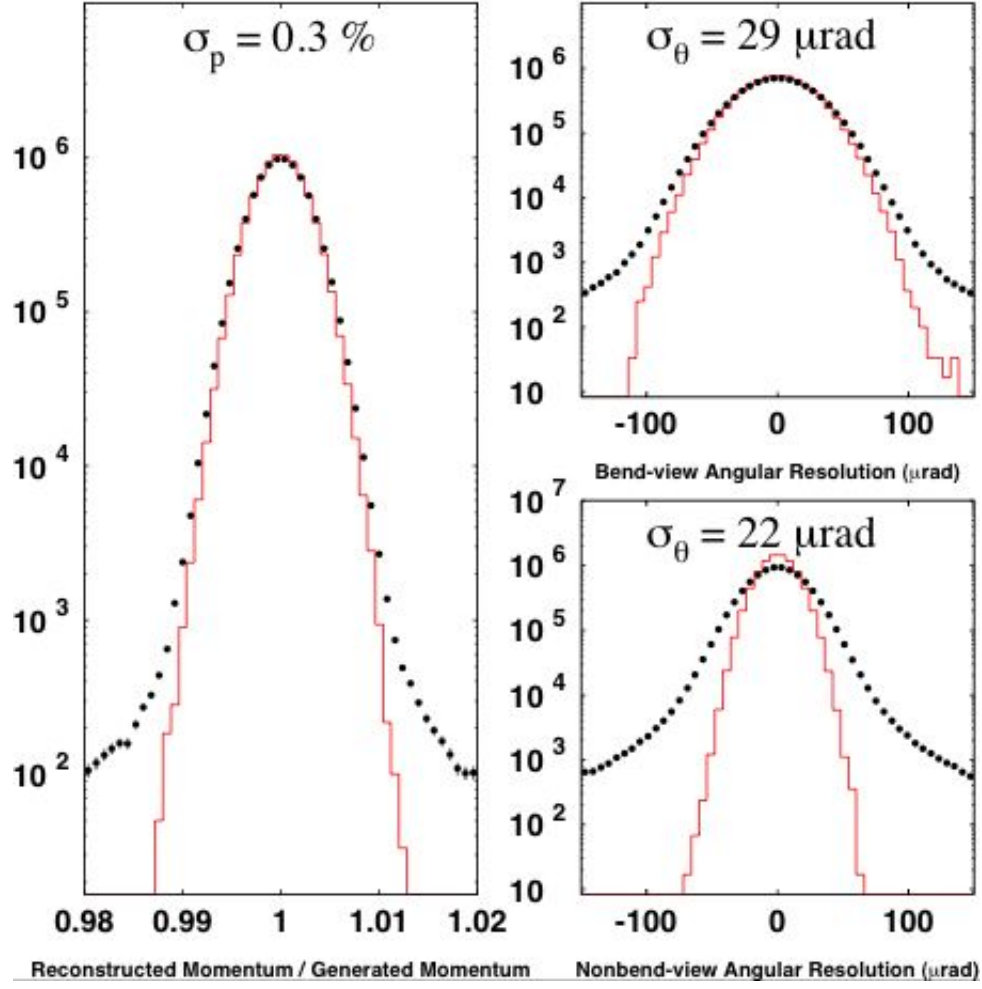
Fig. 5. The momentum and angular resolution of the reconstructed K^+ in the UMS. The tracks were selected to have reduced $\chi^2 < 4$. The dots (histogram) shows the effect with (without) multiple scattering simulation.

Because of the lack of the KEAT and the desire to minimize interactions, the P940 upstream design makes every effort to minimize the Krich material seen by the beam. The beam waist in the Krich is small (1 cm x 1 cm) and goes through a hole in the primary mirror. The Krich gas is H_2 at atmospheric pressure, and so the windows can be made of 1-mil thick kapton.

We can now examine the $K\pi2$ background due to K^+ scattering in the upstream material. Figure 6 shows the M^2_{miss} when the K^+ is subjected to scattering in the upstream
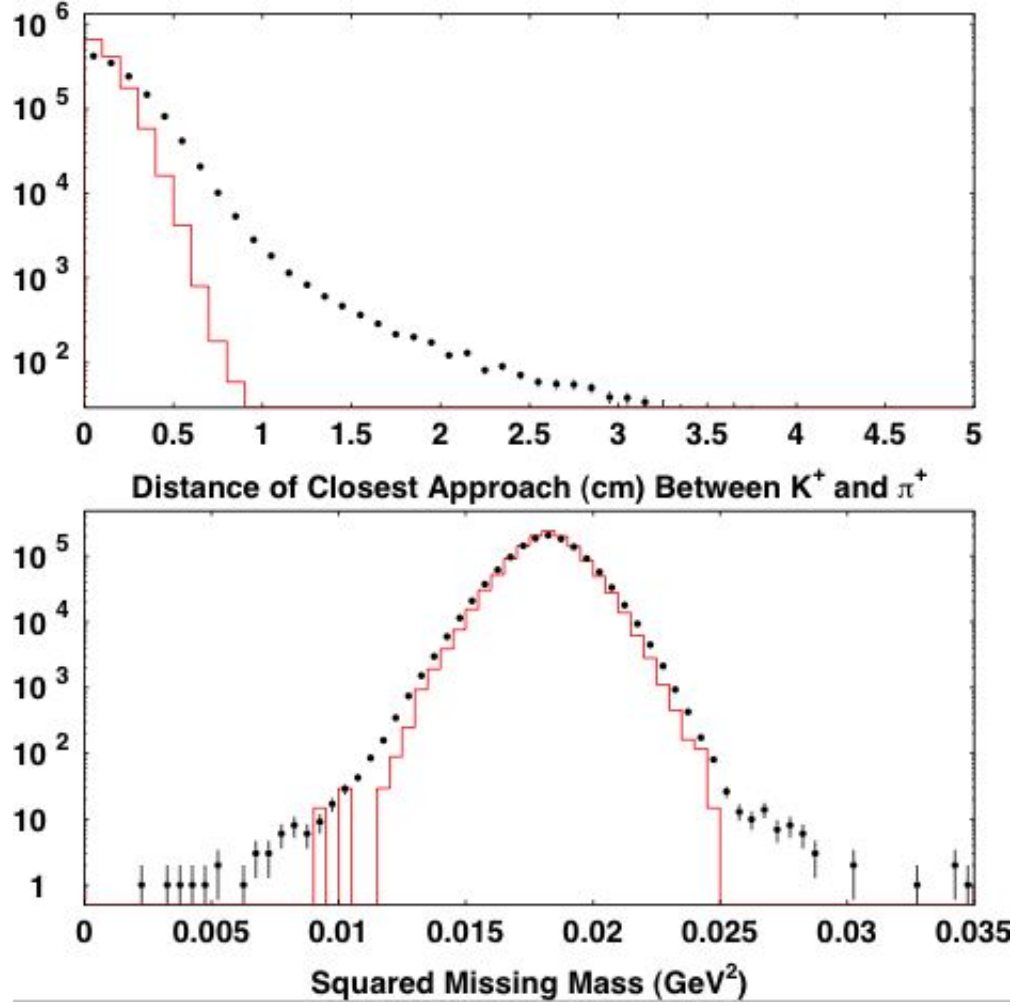
9

Fig. 6. The Distance of Closest Approach (DOCA) and the M_{miss}^2 for $K\pi2$ events. The dots (histogram) shows the quantities with (without) multiple scattering simulation. For the simulation of the π^+ response, only gaussian detector responses were simulated (i.e. no multiple scattering in DMS or Prich).

material. The events satisfy $p_\pi > 13$ GeV/c, $\theta_\pi > 6$ mrad, and DOCA < 1 cm. For the simulation of the π^+ response, only gaussian detector responses were simulated (i.e. no multiple scattering in DMS or Prich).

As shown in figure 6, the number of events in region I, defined as $-0.004 < M_{miss}^2 <$

0.008 GeV^2, is 14 events out of 1.3M events. This represents a region I kinematic rejection factor of $(1.1 \pm 0.3) \cdot 10^{-5}$ events. We can now examine which of the upstream material is contributing to the background. For these events, figure 7 shows the p_t imparted by the upstream material. The p_t of the scatters are in the range 20-40 MeV/c. There is also no single dominant scattering source.

4.2   Accidental Effects

The UMS must be able to track the K^+ in a 230 MHz beam. A simulation and pattern recognition package is used to evaluate K^+ tracking in this high rate environment. The goal is to determine the tracking efficiencies and mistakes in the K^+ reconstruction. These mistakes are propagated into a $K\pi 2$ simulation, where we evaluate how often these mistakes cause the $K\pi 2$ to become background to $\pi^+ \nu \bar{\nu}$. The multiple scattering was not simulated, so that the effect of accidentals could be studied in isolation.

The overall strategy goes as follows. A K^+ track will trigger the KRICH, and deposit hits in the UMS. The pattern recognition must sift through all the extra UMS hits that are present due to the other tracks. Therefore, the first step in the simulation is to determine how many extra tracks to generate, and their arrival times at the UMS chambers. The simulation assumes a beam free of micro time-structure. In the next step, we simulate the UMS hits (space and time) due to each track. We make the UMS hit simulation as realistic as possible. Next, the UMS hits from all tracks are merged into a single event record. The event record is processed by a pattern recognition and fitting program, in which we evaluate the efficiencies and tracking corruptions. In the final step, these tracking results are propagated into a $K\pi 2$ simulation, where we evaluate how often the corruptions can cause $K\pi 2$ to become $\pi^+ \nu \bar{\nu}$ background.
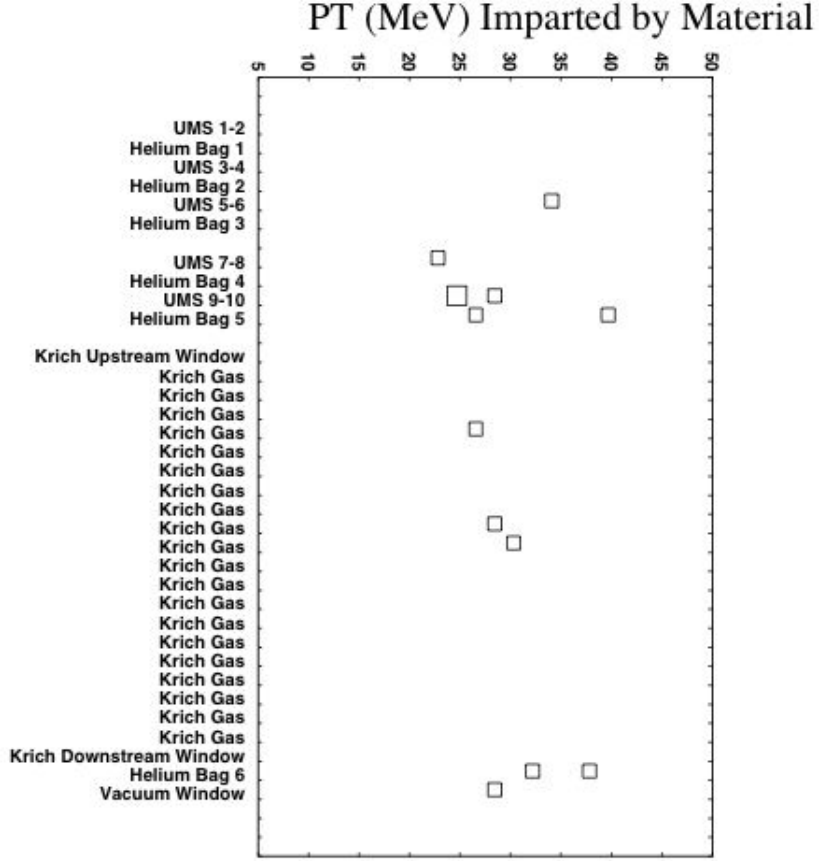
Fig. 7. For the $K\pi2$ events that scatter in the upstream material, and become background in the Region-I signal region, the figure shows the p_t (MeV) imparted by the material.

4.2.1 Generation of Track Multiplicity and Times

The KRICH trigger determines when the K^+ track arrived at the target (t_0). An event is defined as a set of UMS hits consistent with being intime with the KRICH trigger. A UMS

hit (t_{hit}) is defined as being intime if it satisfies:

$$t_0 + t_{flight} + T_{drift}^{MIN} < t_{hit} < t_0 + t_{flight} + T_{drift}^{MAX} \qquad (2)$$

The value t_{flight} is simply the flight time from the target to the UMS station in question. The values T_{drift}^{MIN} and T_{drift}^{MAX} are the minimum and maximum possible drift times of the ionized electrons. These values depend on the location of the drift-view of the beam centroid and width, and on the drift velocity of the gas. This is diagrammed in figure 8. The simulation
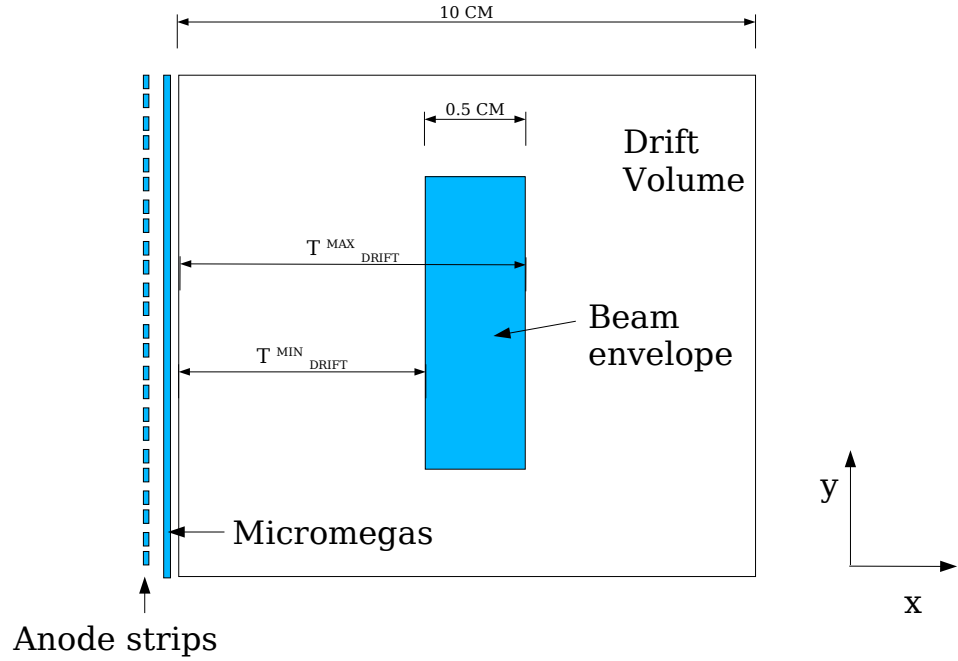

Fig. 8. Minimum and maximum drift times in a UMS chamber. Given a drift velocity of 100 μm/nsec, T_{drift}^{MIN} and T_{drift}^{MAX} are 475 nsec and 525 nsec respectively.

uses an electron velocity in CF$_4$-ethane is 100μm/nsec, a chamber drift dimension of 10 cm, a beam that is centered in the drift view, and a beam width of approximately 0.5 cm in all

13

UMS chambers. [2] Therefore, we have:

$$T_{drift}^{MIN} = \frac{47500 \ \mu m}{100 \ \mu m/nsec} = 475 \ nsec \qquad T_{drift}^{MAX} = \frac{52500 \ \mu m}{100 \ \mu m/nsec} = 525 \ nsec$$

The time window of $T_{drift}^{MAX} - T_{drift}^{MIN} = 50$ nsec allows for accidental tracks to deposit hits that can be considered to be intime. For example, a track arriving 50 nsec earlier than t_0 can deposit an intime hit if the hit drift time is T_{drift}^{MAX}. This happens if the track hits the outer edge of the beam envelope. Similarly, a track arriving 50 nsec later than t_0 can deposit an intime hit if the hit drift time is T_{drift}^{MIN} (inner edge of beam envelope). Therefore, to simulate the proper amount of extra hit activity, we simulate random tracks that strike the target within ± 50 nsec of t_0.

In a time window of ± 50 nsec centered about the K^+ track, there are an average of 23 tracks distributed randomly without microstructure. The K^+ arrival time at the target can be set to $t_0 = 0$ nsec, without loss of generality. After this change, the target arrival time of the other tracks can be determined. The target arrival time of all tracks, after setting the K^+ arrival time to $t_0 = 0$ nsec, is shown in figure 9.

4.2.2 UMS Hit Simulation and Hit Merging

This section describes the simulation of UMS hits for single tracks, and the overlay procedure. The UMS response to single tracks are parameterized from the August 2004 test-beam data of the NA48/2 Kabes system[4]. The Kabes anode strip currents were amplified, discriminated, and sent to a TDC system in which both the leading and trailing times were digitized. A few of the amplified signals were also sent to 500 MHz FADC's. The apparatus included a mixture of 50 μm and 25 μm gap micromegas. We use data from only the latter.

A sample of charged tracks were cleanly identified in low-intensity data. From this

---

[2] The simulation uses a beam divergence of 100 μrad x 100 μrad. Given that the Z-location of the last UMS station is about 50 meters, the beam width is 0.5 cm
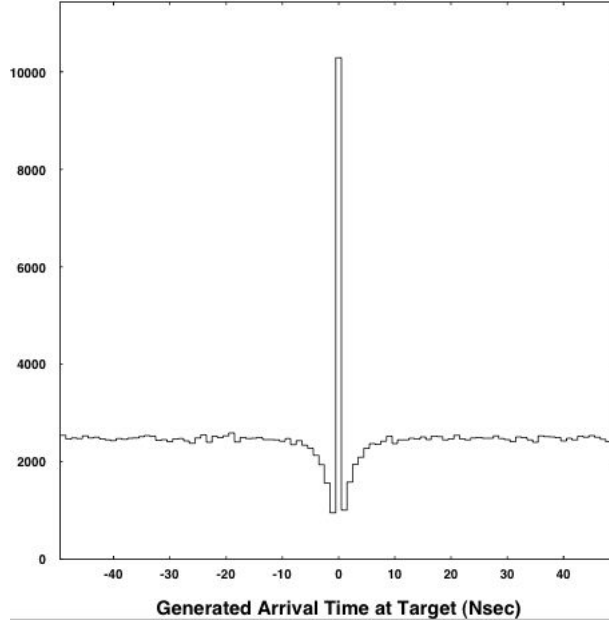
Fig. 9. The time of arrival of all tracks at the target. The K^+ track arrival time is set to $t_0 = 0$ nsec (spike at 0 nsec), without loss of generality.

sample, we measured the strip multiplicity and pulsewidth distributions, and the time resolutions. The strip multiplicity refers to the number of strip hits per track in a single UMS chamber. It reflects the cluster-size of the ionization, and is controlled by effects such as gaseous diffusion and strip pitch. Figure 10 shows the multiplicity to be either 1 or 2 strips. The pulsewidths are simply extracted from the difference between the leading and trailing edge TDC measurements (figure 11).

The time resolutions were measured using events in which a single track deposits charge on an adjacent pair of strips (doublets). In particular, the time difference between the hits on these strips (figure 12) has a mean of zero, but the variation is depends on the intrinsic hit's time resolution. For the 25 μm gap micromegas, the intrinsic time resolution per hit is about 1 nsec, and the dependence on pulsewidth is negligible. As shown in the figure, we also model the non-gaussian tails of the time resolution. The hit efficiency was essentially
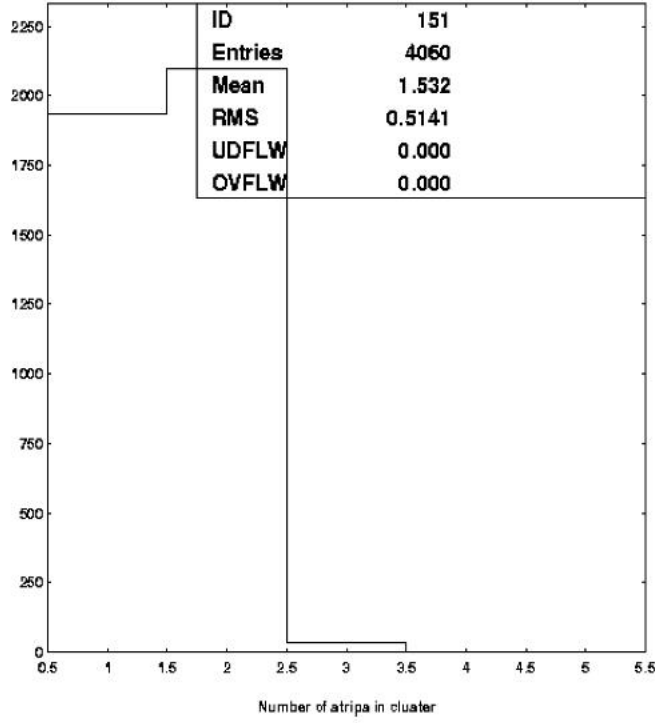
15

Fig. 10. The number of strip hits per track in a single UMS chamber (strip multiplicity).

100% and so did not require a detailed modeling.

To summarize, for each track we generate a track time according to figure 9, and then generate the track hits according to figures 10, 11, and 12. An event is defined as the record of all hits from all tracks. If there are two hits on a strip that are sufficiently close in time, then a simple procedure is used to decide whether to merge the two hits into one. Let t_L^1 (t_L^2) and t_T^1 (t_T^2) be the leading and trailing edges of hit 1 (2). If $t_T^2 < t_L^1$, then the two hits are merged into a single hit of leading edge t_L^1 and trailing edge t_T^2.

4.2.3   UMS Pattern Recognition and Fitting

This section describe the tracking algorithm. Readers can simply skip to the next section to see the tracking results. The most important thing to keep in mind is that the

16

χ²/ndf	173.4	l	26	
Constant		438.3 ±		8.321
Mean		16.91 ±		0.1358
Sigma		8.647 ±		0.1159

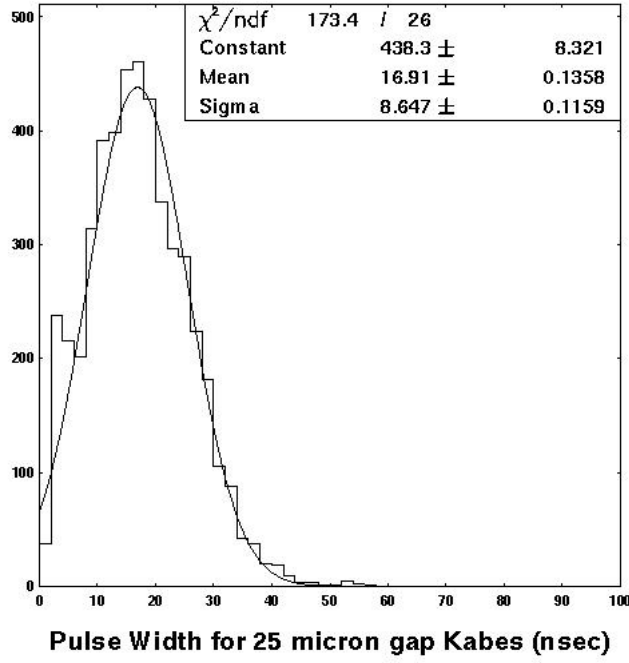**Pulse Width for 25 micron gap Kabes (nsec)**

Fig. 11. The pulsewidth distribution (nsec), defined as the time difference between the leading and trailing TDC edges. The gaussian fit shows our simulation, and we constrain the simulated pulsewidth to exceed 5 nsec.

tracking reconstruction relies heavily on our knowledge of the beam phase space.

Since the event hit multiplicity is rather large, the pattern recognition has to be kept simple and robust. A track in the UMS is described by 6 parameters: 5 track spatial parameters consisting of x_0, θ_x, y_0, θ_y, p, and the event time t_0. Given an arbitrary set of these 6 parameters, one can make a prediction of the strip and leading edge[3] time coordinates of each hit in each UMS chamber. If there exist a hit that agrees with the space and time predictions within resolutions, then it is entered into an array of 'candidate hits'. The track fitting procedure is simply to use the candidate hits and invert a 6x6 matrix and to obtain

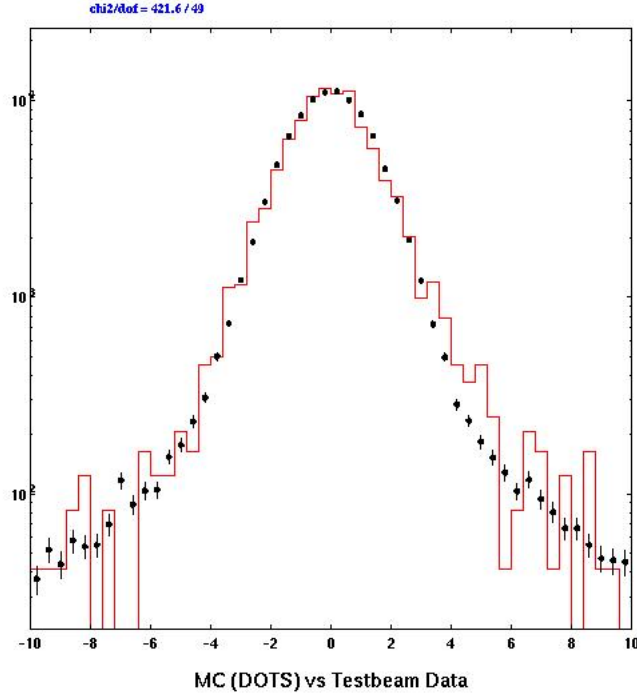[3] In principle, we can predict trailing edges as well.

17

Fig. 12. The time difference (nsec) between hits in a doublet (see text). The intrinsic time resolution per hit is approximately 1 nsec, with negligible pulsewidth dependence. The histogram (dots) shows the data (simulation).

a fit χ^2. In principle, one can scan over all possible parameters in this 6d space, and find all tracks. This would be a simple and robust procedure. It is brute-force, since there is actually no pattern recognition being done.

The pattern recognition that we shall use is similar to this brute-force procedure, but we take advantage of our apriori knowledge of the beam phase space and the KRICH time in order to reduce the space of the parameter scanning. The KRICH gives the t_0. Since the tracks come from a point source, x_0 and y_0 can be taken to be the coordinate of the secondary target. The parameter θ_y affects the strip coordinate. But since the beam divergence is rather small (100 μrad), and the strip pitch is 1 mm, we effectively scan over θ_y by allowing candidate hits

18

to be $\pm$ 3 strips within the prediction of $\theta_y = 0$. So the 6d search space has been contracted to a 2d search space, leaving only θ_x and p.

The 2d scan over θ_x and p is simplified further by using hits in UMS1 as 'seed' hits. In other words, we do not need to search over all possible θ_x and p, but only those parameters that would predict the strip and time coordinates of the UMS1 hit. Given the drift time of a hit in UMS1, we can predict a θ_x since we have t_0 (from the KRICH) and x_0 (point source beam). Given the strip coordinate of a hit in UMS1, we predict p by using the knowledge of y_0 (point source beam), the assumption of $\theta_y = 0$, and the achromatic beam optics.

To summarize, a track is described by 6 parameters, which predicts the strip and time coordinates of hits in all UMS chambers. The task of the pattern recognition is to make an array of hits (candidate hits) that agree with the predictions within resolution. By using the knowledge of the beam phase space and modest assumptions, the number of unknown parameters is reduced to 2 (θ_x and p). Next, we recognize the fact that a hit in UMS1 can be used to predict θ_x and p. So a hit in UMS1 is used to predict the 5 parameter values (t_0 is already given by the KRICH), which in turn predict the strip and time coordinates in the remaining UMS chambers. The array of candidate hits is formed by hits whose strip and time coordinates agree with the prediction within resolution.

The candidate hits are sent to a track fitter, which inverts a 6 x 6 matrix to re-extract the 6 parameters: 5 track spatial parameters consisting of x_0, θ_x, y_0, θ_y, p, and the event time t_0. Since the bend view is orthogonal to the drift view, the problem reduces to inverting two 3 x 3 matrices. The inversion of one 3 x 3 matrix extracts t_0, x_0, θ_x, and χ_1^2. The inversion of the other 3 x 3 matrix extracts y_0, θ_y, p, and χ_2^2. The total χ^2 is simply $\chi_1^2 + \chi_2^2$.

The final crucial step is to refine the list candidate hits using Chavenet's criteria. With very high hit multiplicities, the candidate hit list will contain hits from different tracks. A hit is removed from the candidate hit list if its χ^2 contribution exceeds 5. The candidate hit list

is refitted to get updated track parameters and the fit χ^2. One searches again for hits that have $\chi^2 > 5$, and remove them from the candidate hit list. The candidate hit list is refitted yet again. The procedure terminates when no hits can be removed from the candidate hit list. We declare a track to be found if there are at least 7 hits, with the overall reduced $\chi^2 < 8$, and χ_1^2, $\chi_2^2 < 4$.
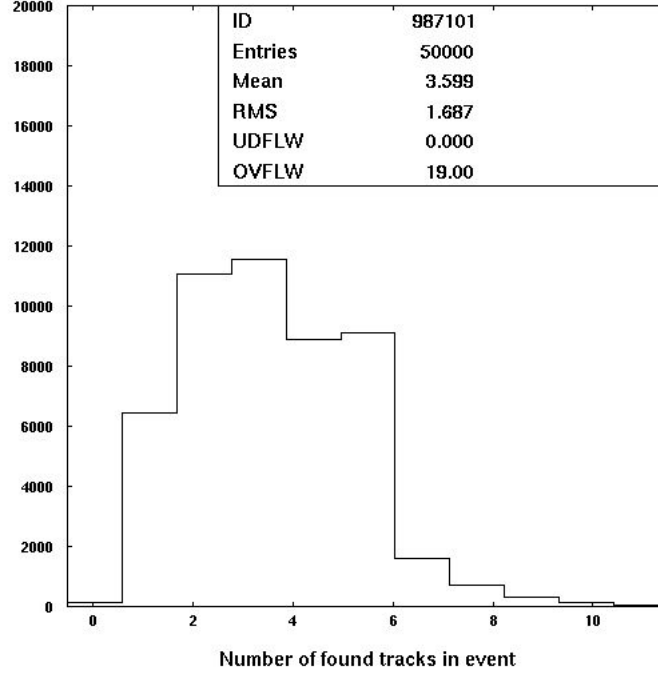

Fig. 13. Distribution of the number of tracks found per event.

4.2.4   Tracking Results

The pattern recognition finds a number of tracks in an event (figure 13). These include the K^+ track itself, other tracks that happen to be coincident in time with the K^+ tracks, and ghost tracks (exact definition given later). Given that many UMS tracks will be found in each event, there is no obvious additional UMS information to decide which track is the K^+ track. Information is used from the KRICH and DMS detectors to select the best possible

track. This is a substantively different situation than in CKM.

Examining the list of tracks found in a given event, the pattern recognition finds the K^+ track with 90% efficiency at an instantaneous charged particle rate of 250 MHz. Figures 14 and 15 shows the reconstructed t_0 and momentum resolution of the K^+ track. The non-gaussian momentum tails are due to accidental hits. These are cases where the reconstructed track has the majority of its hits from the geniune K^+ track, and a minority of hits from other tracks.
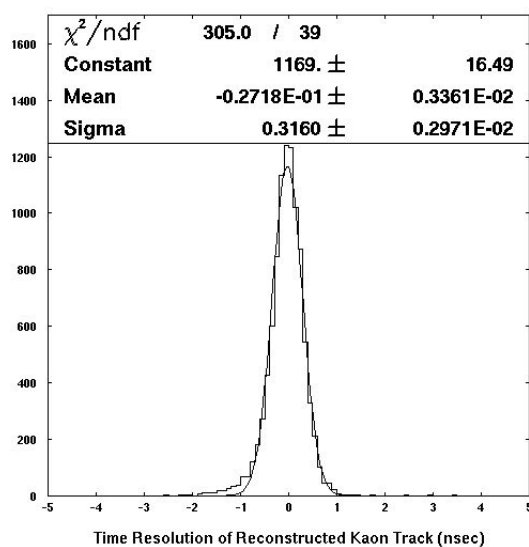

Fig. 14. The reconstructed time (nsec) of the K^+ tracks, where the simulated time was 0 nsec.

Since the average number of found tracks is 3.5 per event, the average number of extra tracks is 2.5 per event. The extra tracks are predominantly ghost tracks in which the reconstruction has combined hits from two real tracks that deposited charge on the same set of strips. In particular, the ghost tracks are formed by combining hits from one real track that drift in the $+x$ direction, with hits from another real track that drift in the $-x$ direction. The real tracks that contribute to ghost tracks can come from $\pm$ 50 nsec of the K^+ track.
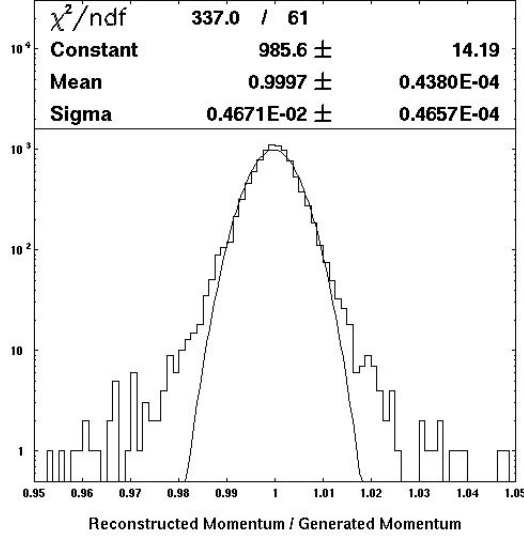
Fig. 15. The ratio of reconstructed K^+ momentum to generated momentum. The nongaussian momentum tails is clearly seen.

Figures 16 and 17 show the reconstructed time and momentum resolution of all found tracks per event.

Of all the tracks found in an event, most of which are ghost tracks, we select the 'best' K^+ track, which is the track whose reconstructed time and momentum best matches the KRICH. The KRICH is simulated to have a 1% gaussian momentum resolution. The selection results in figure 18. In principle, the problem of ghost tracks can be reduced by adding additional UMS chambers at stereo angles, or by a plane of pixels where each hit gives an x, y and t information. These options are under study.

4.2.5 Effect of High Rate Environment on $K\pi2$

Finally, we can now evaluate the effect of the high rate environment on the $K\pi2$ background. The background mechanism is where the K^+ is mismeasured, and would cause the M^2_{miss} of $K\pi2$ events to migrate into the signal region. As described in the previous
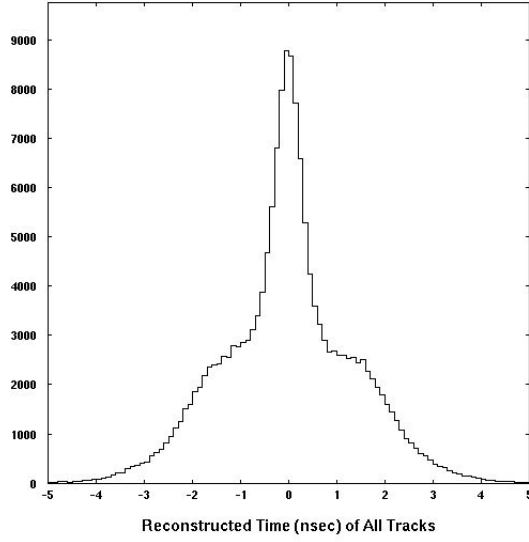
Fig. 16. The reconstructed time (nsec) of all tracks found in the event. The K^+ tracks show up as the sharp peak at 0 nsec. The broader background are predominantly due to ghost tracks (see text).

subsection, the mismeasurement are due to (1) a minority of accidental hits corrupting an otherwise well reconstructed track (see figure 15), or (2) that a ghost track was used instead of the correct K^+ track.

Figure 19 shows the DOCA and M^2_{miss} of $K\pi2$ events, in the 250 MHz charged particle rate environment. The reconstruction without high rate effects are also shown, for comparison. We have required $p_\pi > 13$ GeV/c, $\theta_\pi > 6$ mrad, and DOCA < 1 cm. For the simulation of the π^+ response, only gaussian detector responses were simulated (i.e. no multiple scattering in DMS or PRICH). We note that the DOCA requirement reduces the ghost track problem somewhat.

In region I, 8 out of 637401 events remain. This represents a kinematic rejection of $(1.3 \pm 0.4) \cdot 10^{-5}$.
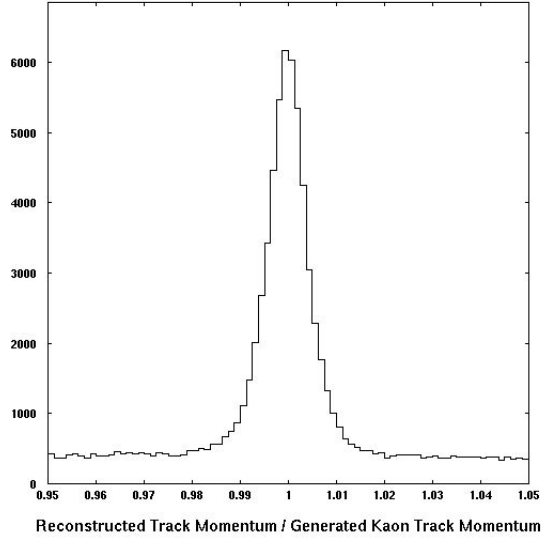
23

Fig. 17. The ratio of reconstructed track momentum to the generated K^+ momentum. The broad flat background is due to ghost tracks.

5 Conclusion

This document presented the proposed layout of the P940 Upstream Magnetic Spectrometer. The technology is based on a 25 μm gap micromegas TPC, such as the NA48/2 Kabes system. The effect of multiple scattering, including material in all upstream detectors, has been simulated. The resulting $K\pi2$ background, due to multiple scattering effects corrupting the UMS K^+ measurement is evaluated. The region-I kinematic cuts reject $(1.1 \pm 0.3) \cdot 10^{-5}$ $K\pi2$ events.

The effect of UMS tracking in a 250 MHz rate environment has been evaluated. Simulated events consist of overlays of approximately 25 single tracks, where the beam is simulated without micro time-structure. The UMS response to single tracks is taken from the August 2004 NA48/2 testbeam data.

The pattern recognition reconstructs generated tracks with 90% efficiency. It relies
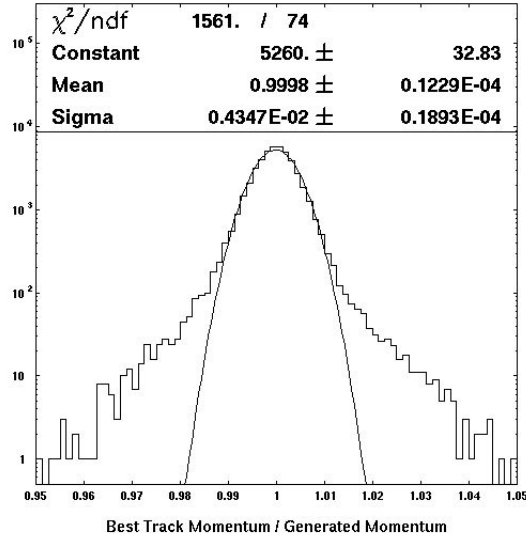
Fig. 18. The ratio of the best reconstructed track momentum to the generated K^+ momentum. The reconstruction usually finds 3.5 tracks per event at 250 MHz charged particle rate. The track that best matches the KRICH time and momentum measurement is selected.

heavily on the knowledge of the beam phase space. It finds an average of 2.5 extra tracks per event, in addition to the K^+ track. The extra tracks are primarily ghost tracks. They are removed by checking against the KRICH time and momentum measurement, and the DOCA quality. The resulting $K\pi2$ background in region-I, where the K^+ measurement has been corrupted by the 250 MHz environment, is $(1.3 \pm 0.4) \cdot 10^{-5}$.

References

[1] Bernard Peyaud, contribution to the Vienna Conference on Instrumentation, February 2004.

[2] There is a tremendous amount of literature on Micromegas. See for example the seminal paper by Y. Giomataris, NIM **A419** (1998) 239-250.

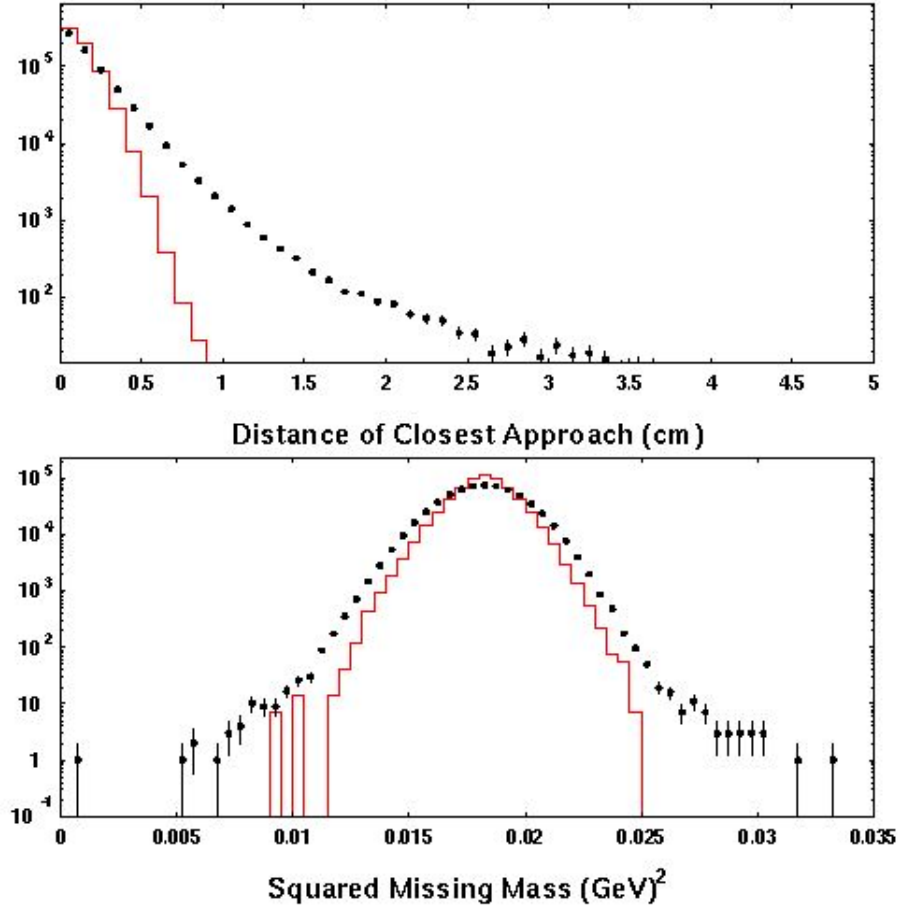[3] Figure courtesy of E. Mazzucato of the Saclay, NA48 collaboration.

25

Fig. 19. The Distance of Closest Approach and M_{miss}^2 for $K\pi2$ events. The dots (histogram) show the recontruction with (without) the 250 MHz charged particle environment.

[4] NA48/2 Testbeam Memo to be written.